Variable xy-UV beam expander for high-power laser beam shaping

Georg Nadorff [a], Frank DeWitt IV [a], Sten Lindau [b]
[a] Melles Griot, 55 Science Parkway, Rochester, NY 14620
phone +1 585 244-7220; email mgoptics@idexcorp.com
[b] Micronic Mydata AB, Nytorpsvägen 9, SE-18303 Täby, Sweden

This paper was published in Proc. SPIE Vol. 8490, *Laser Beam Shaping XIII*, edited by Andrew Forbes, Todd E. Lizotte, 84900I (2012)
doi: 10.1117/12.929744; http://dx.doi.org/10.1117/12.929744

Variable xy-UV beam expander for high-power laser beam shaping

Georg Nadorff*[a], Frank DeWitt IV[a], Sten Lindau[b]
[a]CVI Melles Griot, 55 Science Parkway, Rochester, NY 14620;
[b]Micronic Mydata AB, Nytorpsvägen 9, SE-18303 Täby, Sweden

ABSTRACT

A five element zoomable anamorphic beam expander is designed and fabricated for a laser illumination system used in the manufacture of patterned micro-circuit substrates. The beam expander is the front end of a Gaussian to top-hat beam shaping illuminator. The tightly toleranced optical system downstream of the beam expander should not be readjusted with changes to the input beam. The job of the beam expander is to maintain, independent of the input beam, a constant diffraction limited output beam size as well as a specific waist location. A high power quasi-CW laser at 355 nm is employed for high throughput. The specifications of the laser allow for a range of x,y-beam diameters (ellipticity), x,y-waist locations (astigmatism), and x,y-divergence. As the laser's frequency tripling crystal is exposed to high fluence over time, the beam parameters will change. At some point the laser is exchanged for a new one, and a new set of beam parameters is presented to the beam expander. Movable cylindrical lenses enable the independent adjustment of x- and y-beam parameters. The mounting cells are motorized to enable adjustments remotely. We present the optical design approach using Gaussian beam ray tracing and discuss the mechanical implementation.

Keywords: Beam expander, cylindrical anamorphic, beam shaping, Gaussian beams, variable motorized zoom, UV, LDI

1. INTRODUCTION

Laser direct imaging (LDI) is a key technology enabling the high volume production of advanced micro-circuit boards and patterned substrates.[1] With LDI, a pattern of interconnects is transferred directly to the substrate from a digital format without the need for a photomask, as is employed in traditional lithography. LDI offers advantages over traditional lithography in meeting three key process parameters simultaneously: the abilities to write small structures, to achieve extremely precise correlation between the different layers, and to produce copies at high speed.

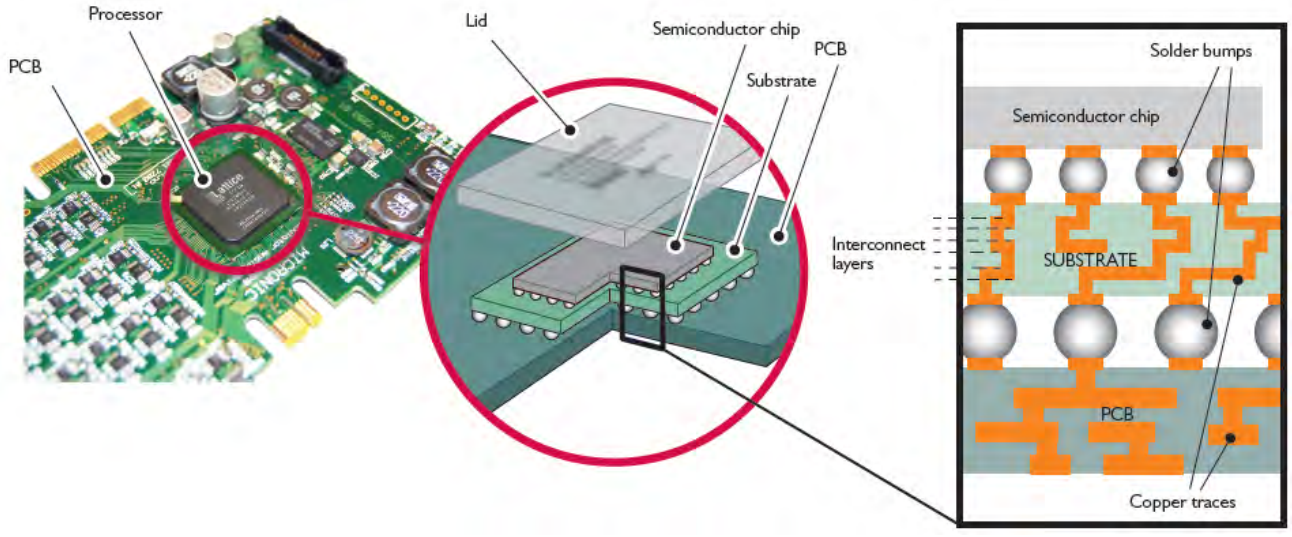

Figure 1. LDI processing is used to create multiple layers of copper trace interconnections in substrates that connect semiconductor chips to printed circuit boards (PCBs). Such PCB assemblies are integrated in smart phones, tablets, or computers. As the performance of these devices continually increases, the demands on complexity, packing density, and critical dimensions of the multilayer interconnects follow suit.

* gnadorff@cvimellesgriot.com; phone +1 585 241-2280; www.cvimellesgriot.com

Laser Beam Shaping XIII, edited by Andrew Forbes, Todd E. Lizotte, Proc. of SPIE Vol. 8490, 84900I

1.1 Overall architecture

The LDI optical system contains an illumination module and a projection module. The job of the illumination module is to convert a Gaussian laser beam to a top-hat diffraction limited intensity distribution. This intensity distribution illuminates a spatial light modulator (SLM) which provides the digital pattern to be relayed by the projection system onto a photo resist coated copper clad plate, from which the substrates will eventually be diced. The illumination optical system consists of many sub-systems to be able to present the required top-hat distribution onto the SLM. In this paper we focus on only one of these sub-systems, a variable x,y-beam expander.

1.2 Light source

The latest generation of tools employs quasi-CW mode-locked diode pumped solid-state (DPSS) lasers.[2,3] Because of the need for high throughput, the higher the laser's power, the faster the patterns can be printed. Because of the need for smaller printed dimensions, DPSS lasers have been developed to operate in the ultraviolet (UV). One of the technical hurdles in employing a high power UV laser in a tool which is intended to operate continuously 24/7 for many years is that the laser beam characteristics can drift, or worse, degrade over time. UV lasers tend to be self-destructing, and despite internal monitoring and crystal compensation, they are never 100% stable. For a finely tuned diffraction limited optical system, such input beam drift can be detrimental to the imaging performance. In the worst case, the laser needs to be replaced after its power has dropped below an irrecoverable threshold, in which case the new laser may have entirely different beam parameters than its predecessor had.

1.3 Variable beam expander

Because the total LDI optical system is extremely complex, the goal is to not require any adjustments once the system has been calibrated and brought online. This requirement is met by using a variable beam expander positioned directly between the output zone of the laser and the input to the remaining illumination system. As the laser beam parameters change, the beam expander is zoomed to compensate, such that its output remains constant, regardless of input. The beam expander must be designed to cover the full range of possible beam parameters which are guaranteed by the laser manufacturer.

2. DESIGN SPECIFICATIONS

2.1 Laser beam characteristics

The specific laser output beam parameters are published by the manufacturer in two separate locations.[3,4]

Table 1. Paladin Advanced 355 laser beam specifications from Refs [3] and [4]. What is noted as "beam diameter" in Ref [4] is in fact the "beam waist diameter" to be consistent with Ref [3]. Ref [3] is essential as it specifies the waist location.

LASER BEAM PARAMETERS

Wavelength	355 nm
Output power	> 16 W
Beam quality M^2	< 1.2
Beam waist diameter	1.35 mm +/- 15%
Beam divergence	340 µrad +/- 15%
Rayleigh Range	~ 4 m
Beam waist location	-0.1 m +/- 35% of RR
Astigmatism	< 50% of RR
Ellipticity	0.85 – 1.15

Paladin™ Advanced 355
Modelocked UV Laser

Wavelength (nm)	355
Output Power[1] (W)	
Paladin Advanced 355-8000	>8
Paladin Advanced 355-10000	>10
Paladin Advanced 355-16000	>16
Repetition Rate (MHz)	80 ±1 MHz
Pulse Length (ps)	>15 @ 1064 nm
Spatial Mode	TEM_{00}
M^2	<1.2
Beam Diameter (mm)	
Paladin Advanced 355-8000/10000	1 ±15%
Paladin Advanced 355-16000	1.35 ±15%
Beam Divergence (µrad)	<550
Beam Ellipticity	0.9 to 1.1
Pointing Stability (µrad/°C)	<20
Polarization	linear >100:1, vertical
Noise (10 Hz to 2 MHz)	<1% (rms)
Long-term Power Stability	<±2%
Maximum Warm-up Time	<15 min. from standby <1 hour from cold start
Static Alignment Tolerances[2]	
Beam Position (mm)	<±0.5 (x,y)
Beam Angle (mrad)	<±2.5

2.2 Beam expander output beam requirements

The illuminator is responsible for homogenizing the Gaussian beam into a top-hat intensity distribution of specific dimension in x and y, collimation, and wavefront error. Therefore, the illumination system requires that the laser x,y-waists be re-imaged by the beam expander at specific but different locations, and with specific but different x- and y-diameters.

Table 2. Output requirements of beam expander = input requirements for illumination system. The y-waist diameter is always constant, but the x-waist diameter takes on a range of diameters in order to permit independent adjustment of the x-numerical aperture being presented to the projection system.

Parameter	Specification		
y-waist diameter	6.35 mm		
y-waist 1/2-diameter, $w_{0Ry\ out}$	3.175 mm		
y-waist location from laser port	2890 mm		
	low NAx	*med NAx*	*high NAx*
x-waist diameter	6.6 mm	10.5 mm	14.6 mm
x-waist 1/2-diameter, $w_{0Rx\ out}$	3.3 mm	5.25 mm	7.3 mm
x-waist location from laser port	3625 mm		

2.3 Mechanical requirements

The beam expander has the following mechanical requirements as determined by other system considerations:

- Distance from laser port to beam expander = 1052 mm
- Maximum beam expander length < 850 mm
- Independent control of collimation and magnification
- Motorized, remotely adjustable
- Limit sensors for homing and end of range detection

3. OPTICAL DESIGN

3.1 Design method

We will approach the design task by following these steps:

1. Consider the overall layout of the beam expander.
2. Distill the laser specifications from Table 1 to a format tuned to the design task.
3. Restate the requirements in Table 2 together with the laser specifications from Table 1 into a set of clearly defined optical configurations which span the full range of beam parameters.
4. Apply Gaussian beam propagation to the laser beam to determine the basic magnification requirements for the beam expander.
5. Establish first order designs which fulfill the magnification requirements defined in Step 4.
6. Optimize the design to meet the full requirements of beam waist sizes and waist positions using Gaussian beam ray tracing.

3.2 Beam expander arrangement

We have the requirement to manipulate the x- and y-beam parameters independently, because from Table 1 we know the input beam can be elliptical in any orientation, and it exhibits astigmatism (the x- and y-waist occur at different axial locations); plus, from Table 2 we know different x- and y-output beam diameters and different re-imaged x- and y-waist locations are required. Could it get much worse? The solution is to use cylindrical lenses. One set of cylinders will be

oriented with the power axis parallel to x, the other set oriented 90 degrees in relation, with the power axis parallel to y. With this arrangement, the effects of the x-beam expander are unfelt by the y-beam expander, and vice versa. Because cylindrical elements are more difficult and costly to fabricate than spherical elements, we want to minimize the number of elements used. In addition, we desire to use standard catalog elements to avoid fabricating custom cylinders, and they must be made of UV grade fused silica for high transmission at 355 nm. Fortunately, the CVI Melles Griot catalog offers a large selection of standard plano-convex and plano-concave cylinders in UV grade fused silica.

A minimum of three elements is needed to produce a variable beam expander which provides control over both magnification and collimation (although in our case re-imaging the waist location is needed instead of pure collimation). Two elements must be zoomed (one for magnification, the other for collimation), while one element can remain stationary. Which element is the stationary one is not critical as far as the optical design is concerned; different but acceptable solutions can be found for when any one of the three elements is chosen to be fixed.

With this insight, we choose to have the stationary element be shared by both the x- and the y-beam expanders. Since it is shared by both, it needs to impart optical power in both x and y, so we might as well define it as a spherical element (as opposed to a toroidal element). Thus, we have determined the minimum number of elements to be four moving cylinders plus one stationary sphere, as depicted in Figures 2 and 3.

We choose to use a Galilean design form (negative-positive) to minimize the overall length. The exact order of which of the first two elements is to be negative in both the x- and the y-beam expanders can be determined empirically. However, we know the output element of a three-element beam expander should be positive, which makes element 3 (the fixed sphere) and element 5 both convex. This means by default element 4 must be negative (concave). We can then choose either element 1 or 2 to be negative, the other being positive. Making element 1 negative will minimize the overall length.

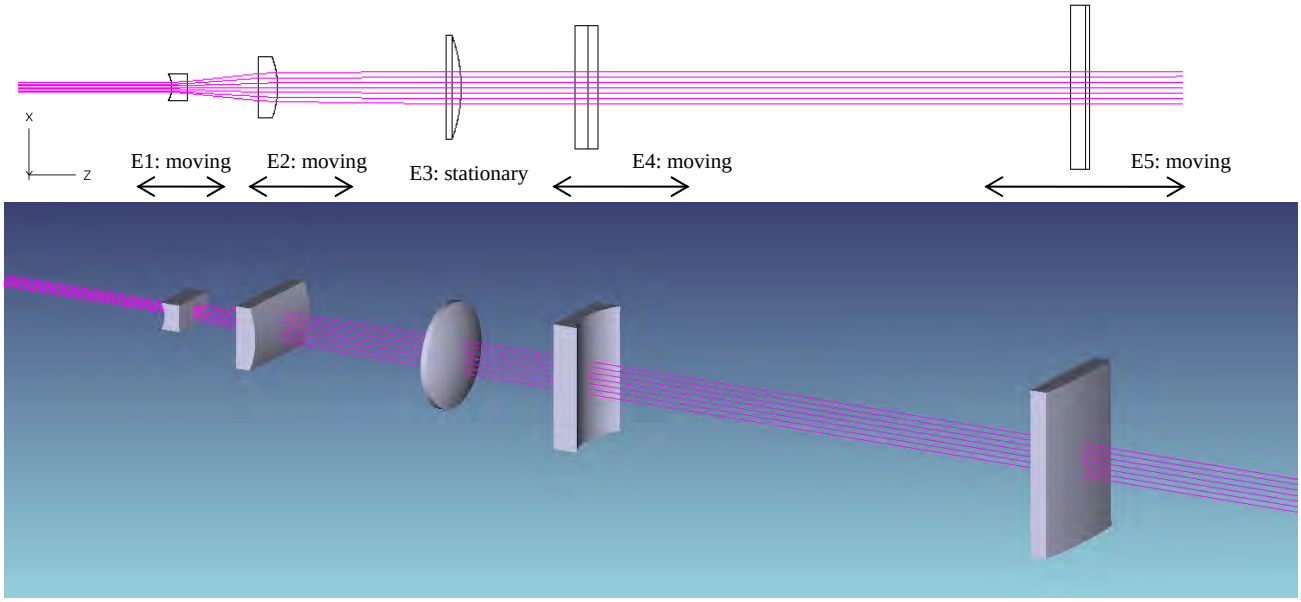

Figure 2. The 5 element x,y-beam expander consists of two moving x-oriented cylinders, a fixed spherical element, and two moving y-oriented cylinders. Note how an x-fan of rays is expanded and collimated by the first three elements (the x-beam expander) and is unaffected by the last two elements.

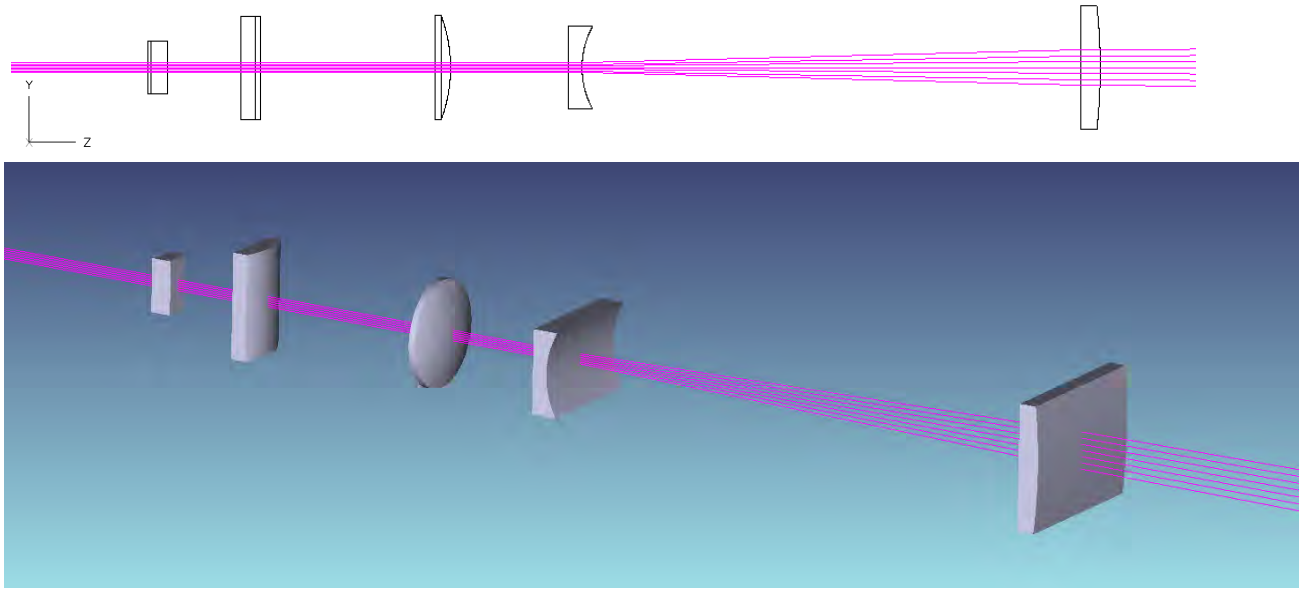

Figure 3. Layout rotated 90° to show how a y-fan of rays is unaffected by the first two elements and is expanded and collimated by the last three elements (the y-beam expander).

3.3 Input beam revisited

To calculate the zoom range needed for the x- and y-variable beam expander(s), we begin with the beam parameters in Table 1. We can recast the range of values to those shown in Table 3 to determine the range of input parameters to the beam expander(s). We omit the beam divergence from Table 1, as it is consistent with the divergence of the Gaussian fundamental TEM_{00} mode and thus does not provide additional information.

Table 3. Laser input beam parameters showing possible min/max values. The Rayleigh Range from Table 1 of 4000 mm is used. The worst case beam diameter is computed as the product of the beam waist diameter and the ellipticity.

Parameter	nominal	+/-		min	mid	max
M^2	1.1	0.1	➔	1.0	1.1	1.2
beam waist diameter (mm)	1.35	15%	➔	1.148	1.350	1.553
beam waist 1/2-diameter, $w_{0\,in}$ (mm)	0.675			**0.5738**	**0.6750**	**0.7763**
laser output port-to-beam waist, $-z_0$ (mm)	-100	1400	➔	**-1500**	**-100**	**1300**
beam ellipticity	1.0	0.15		0.85	1.0	1.15
worst case beam waist diameter (mm)			➔	0.975	1.350	1.785
worst case beam waist 1/2-diameter, $w_{oR\,in}$ (mm)				**0.4877**	**0.6750**	**0.8927**

We see that the potential beam waist diameter in either x- or y- can vary by a factor of (1.785/0.975) = 1.83. In addition, the beam waist can be located (and may move over time) anywhere from 1500 mm inside the laser (i.e. upstream of the laser's output port) to 1300 mm outside the laser (i.e. downstream of the laser's output port).

3.4 Gaussian beams

The beam quality factor, M^2, could be used to compute[5] the "real" beam waist ½-diameter, w_{0R}, as

$$w_{0R} = Mw_0 . \tag{1}$$

However, we assume the M^2 value in Table 1 already applies to the range of waist diameters quoted in Table 1 and thus does not further increase them.

Similarly, one could incorporate M^2 in computing the Rayleigh Range, thereby also further increasing the range of waist locations. The Rayleigh Range, z_R, is given by[5]

$$z_R = \frac{\pi w_{0R}^2}{M^2 \lambda}, \tag{2}$$

where λ = 0.000355 mm. In this case, z_R increases from 4032 mm to 5332 mm, and the worst case laser output port-to-waist distance increases to 1966 mm inside the laser, and to 1766 mm outside the laser. However, since the Rayleigh Range is also already specified in Table 1, we will not apply equation (2) and be content with the parameters as shown in Table 3.

We can now use Gaussian beam propagation to incorporate the variation in beam waist location into the determination of the zoom ranges needed. We compute[5] the beam waist ½-diameter, w_R, as

$$w_R(z) = w_{0R}\left[1+\left(\frac{z\lambda M^2}{\pi w_{0R}^2}\right)^2\right]^{1/2}, \tag{3}$$

where z is the propagation distance from the location of the waist. The propagation distance will equal the sum of the waist-to-port distance, z_0, plus the distance from port-to-beam expander specified in Section 2.3. Because Tables 1 and 3 show the distance from port-to-waist, which is $-z_0$, we must reverse the sign to define the distance from waist-to-port. Thus, for the x-beam expander, z = -(-z_0)+ 1052, while for the y-beam expander z = -(-z_0)+ 1052 + ~800/2 (to propagate to the stationary element 3).

3.5 Magnification ranges

Using Equation 3 and the values in Tables 2 and 3, we can arrive at the required y-magnification ranges *(magyBE)*. For each input beam size (min, mid, max) we have three waist positions giving the nine basic combinations listed in Table 4.

Tables 4a and 4b. Starting with the range for $w_{0R\ in}$, we compute for the y-beam expander *magyBE* = $w_{0R\ out}/w_R$. The right table is the same as the left, but sorted by ascending *magyBE*.

$w_{0R\ in}$	-(-z_0) waist-to-port	port-to-E3	z	w_R	NAy	$w_{0R\ out}$	magyBE
0.4877	-1300	1452	152	0.489	fixed	3.18	**6.493**
0.4877	100	1452	1552	0.606		3.18	**5.240**
0.4877	1500	1452	2952	0.840		3.18	**3.780**
0.6750	-1300	1452	152	0.675		3.18	**4.700**
0.6750	100	1452	1552	0.723		3.18	**4.390**
0.6750	1500	1452	2952	0.837		3.18	**3.795**
0.8927	-1300	1452	152	0.893		3.18	**3.556**
0.8927	100	1452	1552	0.914		3.18	**3.474**
0.8927	1500	1452	2952	0.968		3.18	**3.281**

$w_{0R\ in}$	-(-z_0) waist-to-port	port-to-E3	z	w_R	NAy	$w_{0R\ out}$	magyBE
0.8927	1500	1452	2952	0.968	fixed	3.18	**3.281**
0.8927	100	1452	1552	0.914		3.18	**3.474**
0.8927	-1300	1452	152	0.893		3.18	**3.556**
0.4877	1500	1452	2952	0.840		3.18	**3.780**
0.6750	1500	1452	2952	0.837		3.18	**3.795**
0.6750	100	1452	1552	0.723		3.18	**4.390**
0.6750	-1300	1452	152	0.675		3.18	**4.700**
0.4877	100	1452	1552	0.606		3.18	**5.240**
0.4877	-1300	1452	152	0.489		3.18	**6.493**

We see the variable y-beam expander needs to cover the magnification range *magyBE* from 3.281 to 6.493 (which is a ~2x optical zoom). We also see that the largest $w_{0R\ in}$ when combined with the furthest out z_0 yields the lowest *magyBE*, whereas the smallest $w_{0R\ in}$ combined with the closest z_0 requires the largest *magyBE* (which in hindsight is intuitive). If we had used *magyBE* = $w_{0R\ out}/w_{0R\ in}$ instead of *magyBE* = $w_{0R\ out}/w_R$, then we would have been close to correct with the highest *magyBE*, but we would have been incorrect with the lowest *magyBE*.

For the x-beam expander, we define the x-magnification range *(magxBE)* in a similar way. The task is a bit more complex due to the requirement for a varying output beam size. For each of the three input beam sizes (min, mid, max) we have three waist positions at three potential output beam sizes, giving the 27 combinations listed in Table 5.

Tables 5a and 5b. Starting with the range for $w_{0R\ in}$, we compute for the x-beam expander $magxBE = w_{0R\ out}/w_R$. We have the additional complication that $w_{0R\ out}$ will vary. The right table is the same as the left, but sorted by ascending *magxBE*.

$w_{oR\ in}$	-($-z_0$) waist-to-port	port-to-E1	z	w_R	NAx	$w_{oR\ out}$	magxBE
0.4877	-1300	1052	-248	0.491	low	3.30	**6.720**
0.4877	100	1052	1152	0.556	low	3.30	**5.936**
0.4877	1500	1052	2552	0.766	low	3.30	**4.305**
0.6750	-1300	1052	-248	0.676	low	3.30	**4.880**
0.6750	100	1052	1152	0.702	low	3.30	**4.701**
0.6750	1500	1052	2552	0.799	low	3.30	**4.131**
0.8927	-1300	1052	-248	0.893	low	3.30	**3.694**
0.8927	100	1052	1152	0.905	low	3.30	**3.648**
0.8927	1500	1052	2552	0.949	low	3.30	**3.476**
0.4877	-1300	1052	-248	0.491	med	5.25	**10.691**
0.4877	100	1052	1152	0.556	med	5.25	**9.443**
0.4877	1500	1052	2552	0.766	med	5.25	**6.850**
0.6750	-1300	1052	-248	0.676	med	5.25	**7.763**
0.6750	100	1052	1152	0.702	med	5.25	**7.479**
0.6750	1500	1052	2552	0.799	med	5.25	**6.572**
0.8927	-1300	1052	-248	0.893	med	5.25	**5.877**
0.8927	100	1052	1152	0.905	med	5.25	**5.804**
0.8927	1500	1052	2552	0.949	med	5.25	**5.530**
0.4877	-1300	1052	-248	0.491	high	7.30	**14.865**
0.4877	100	1052	1152	0.556	high	7.30	**13.130**
0.4877	1500	1052	2552	0.766	high	7.30	**9.524**
0.6750	-1300	1052	-248	0.676	high	7.30	**10.794**
0.6750	100	1052	1152	0.702	high	7.30	**10.399**
0.6750	1500	1052	2552	0.799	high	7.30	**9.138**
0.8927	-1300	1052	-248	0.893	high	7.30	**8.172**
0.8927	100	1052	1152	0.905	high	7.30	**8.070**
0.8927	1500	1052	2552	0.949	high	7.30	**7.689**

$w_{oR\ in}$	-($-z_0$) waist-to-port	port-to-E1	z	w_R	NAx	$w_{oR\ out}$	magxBE
0.8927	1500	1052	2552	0.949	low	3.30	**3.476**
0.8927	100	1052	1152	0.905	low	3.30	**3.648**
0.8927	-1300	1052	-248	0.893	low	3.30	**3.694**
0.6750	1500	1052	2552	0.799	low	3.30	**4.131**
0.4877	1500	1052	2552	0.766	low	3.30	**4.305**
0.6750	100	1052	1152	0.702	low	3.30	**4.701**
0.6750	-1300	1052	-248	0.676	low	3.30	**4.880**
0.8927	1500	1052	2552	0.949	med	5.25	**5.530**
0.8927	100	1052	1152	0.905	med	5.25	**5.804**
0.8927	-1300	1052	-248	0.893	med	5.25	**5.877**
0.4877	100	1052	1152	0.556	low	3.30	**5.936**
0.6750	1500	1052	2552	0.799	med	5.25	**6.572**
0.4877	-1300	1052	-248	0.491	low	3.30	**6.720**
0.4877	1500	1052	2552	0.766	med	5.25	**6.850**
0.6750	100	1052	1152	0.702	med	5.25	**7.479**
0.8927	1500	1052	2552	0.949	high	7.30	**7.689**
0.6750	-1300	1052	-248	0.676	med	5.25	**7.763**
0.8927	100	1052	1152	0.905	high	7.30	**8.070**
0.8927	-1300	1052	-248	0.893	high	7.30	**8.172**
0.6750	1500	1052	2552	0.799	high	7.30	**9.138**
0.4877	100	1052	1152	0.556	med	5.25	**9.443**
0.4877	1500	1052	2552	0.766	high	7.30	**9.524**
0.6750	100	1052	1152	0.702	high	7.30	**10.399**
0.4877	-1300	1052	-248	0.491	med	5.25	**10.691**
0.6750	-1300	1052	-248	0.676	high	7.30	**10.794**
0.4877	100	1052	1152	0.556	high	7.30	**13.130**
0.4877	-1300	1052	-248	0.491	high	7.30	**14.865**

In Table 5b we see the variable x-beam expander needs to cover the magnification range *magxBE* from 3.476 to 14.865, which is wider than the y-beam expander needs to cover (a ~4.3x optical zoom). We also see that, as with the y-beam expander, the largest $w_{0R\ in}$ combined with the furthest out z_0 yields the lowest *magxBE*, whereas the smallest $w_{0R\ in}$ combined with the closest z_0 requires the largest *magxBE*. Also here, had we used $magxBE = w_{0R\ out}/w_{0R\ in}$ instead of $magxBE = w_{0R\ out}/w_R$, we would have been close with the highest *magxBE*, but we would have missed slightly the lowest *magxBE*. We also see that both the medium NAx and the middle $w_{0R\ in}$ tend to intermingle with magnifications required for the high and the low NAx.

3.6 First order design for magnification only

We would like to establish a preliminary first order geometrically afocal zoomed three-element design which temporarily ignores the re-imaging of the waist requirement but meets the magnifications summarized in Tables 4b and 5b. We can design the x- and y-beam expanders independently (as spherical elements if we desire) and then combine them at the end, converting elements 1,2,4,5 to cylinders at that time.

Given lens elements 1, 2, and 3 (E1, E2, E3) spaced by distances t_1 and t_2, we can solve the standard thin lens raytracing equations for the power of E2 as a function of the power of E1, t_1, and t_2. Unfortunately, this approach does not lead to a unique solution, even if each element is already pre-defined as either positive or negative. Nevertheless, we can start with the high magnification position, since we know t_1 will be minimized there. We then choose a starting value for both the power of E1 and $t_{1(high\ mag)}$. Then we can compute the powers and separation for E2 and E3. Thereafter the magnification is changed to the low end, and another guess must be made for a new $t_{1(low\ mag)}$. Then the requirement must be met that the powers of E2 and E3 be equal at both zoom positions. There is no analytic solution for this case; it must be found either parametrically or simply by optimization. Since there are four variables involved (power of E1, $t_{1(low)}$, $t_{1(high)}$, and maximum overall length t_1+t_2), navigating 4-D space parametrically is a daunting task, so direct optimization is the better option. We can iterate the design until all requirements are met, making sure to keep the elements only

plano-convex or plano-concave, since as the last step, we require the use of available catalog elements. Thus, once the requirements are met, we find the closest match to a catalog radius of curvature and substitute one at a time, re-optimizing between each substitution.

Table 6. Lens Data Editor spreadsheet in Zemax[8] defining the complete beam expander. All five glass elements correspond to standard CVI Melles Griot catalog components.

Surf:Type		Comment	Radius	Thickness		Glass	Semi-Diameter			Radius of R..
OBJ	Standard		Infinity	Infinity			0.000000			
1	Standard	waist pos	Infinity	1500.0000			0.675000			
2	Standard	laser port	Infinity	1052.0000			0.675000			
3	Standard	M10 to xLBE3=477.5	Infinity	373.51940	T		0.675000			
4*	Toroidal	xLBE 1	Infinity	4.000000		F_SILICA	0.675000			-6.500000
5*	Toroidal	zooming for x	Infinity	18.306941			0.675000			0.000000
6*	Toroidal	xLBE 2	Infinity	5.000000		F_SILICA	0.675000			0.000000
7*	Toroidal	zooming for x	Infinity	76.673658			0.675000			-20.30000
8*	Standard	xLBE3/yLBE1	Infinity	4.000000		F_SILICA	17.000000	U		
9*	Standard	zooming for y	-206.0000	61.166962			17.000000	U		
10*	Toroidal	yLBE 2	Infinity	3.500000		F_SILICA	0.579576			0.000000
11*	Toroidal	zooming for y	20.300000	133.58940			0.575869			0.000000
12*	Toroidal	yLBE 3	Infinity	5.000000		F_SILICA	2.172702			0.000000
*	Toroidal		-127.1000	240.24364	T		2.213036			0.000000
14	Standard	M10 to M9=925	Infinity	913.00000	T		3.093130			
15	Standard	y-waist @ 2890	Infinity	735.00000	T		6.437492			
16	Standard	x-waist @ 3625	Infinity	0.000000			9.129831			

3.7 Final optimization for beam waist sizes and waist positions using Gaussian beam ray tracing

Once the preliminary design is obtained, we then require the re-imaging of the waist at the precise locations specified in Table 2. In this case, geometric ray tracing equations no longer apply, and Gaussian raytracing equations[6,7] must be used instead. Fortunately, the Gaussian raytracing equations are built-in to all modern optical design software, so there is in need to perform this manually.

We found the optimization to be most convenient in Zemax[8], because the merit function accesses the "Skew Gaussian Beam" feature and has predefined operands for directly targeting a Gaussian beam size, waist size, or waist position (operands GBSS, GBSW, and GBSP, respectively). The operands accept as input:

- In#: surface number to start the propagation. In our case this is Surface 2 which represents the laser output port.
- Out#: surface at which to compute the Skew Gaussian Beam data. In our case this is either Surface 16 or 15 at 3625 mm from the laser port for x-, and 2890 mm from the laser port for y-, as given in Table 2.
- Wave: wavelength number to use.
- StoW: starting surface to waist distance in lens units. We can keep this either at 0 if we define $-z_0$ (from Table 3) with Surface 1, or put in $-z_0$ here directly if we keep Surface 1 at 0.
- w0: input beam waist ½-diameter in lens units. In our case we will need $w_{0R\,in}$ from Table 3.

Moreover, if w0 is positive, then the computation is for the y-direction beam; if negative, it is for the x-direction. This is important to us, since we must target the x- and y-beam waists independently.

For the x-beam expander we define 27 configurations corresponding to the sorted parameters in Table 5b. Configuration 1 represents the lowest, configuration 27 the highest x-magnification. For the y-beam expander we define 9 configurations corresponding to the sorted parameters in Table 4b. Configuration 1 represents the lowest, configuration 9 the highest y- magnification.

Table 7. Merit Function spreadsheet in Zemax showing the outer configurations 1 and 27 for the x-beam expander. The magnification is monitored as both the ratio in focal lengths, as well as the ratio of the geometric input and output beam diameters. The GBSS operands target the Gaussian beam ½-diameter on surface 16, which is the required location for the re-imaged x-beam waist. If we also use the GBSW operands which target the actual Gaussian beam waist ½-diameter and require that GBSS = GBSW, this forces the waist to occur at surface 16. In addition, we can target the GBSP operand, which is the actual Gaussian beam waist position, to coincide directly on surface 16. Due to the highly non-linear nature of Gaussian beam propagation, we found that forcing GBSS = GBSW is more effective initially than targeting GBSP. However, once GBSS = GBSW, there can still be a minor offset to the desired waist position, and then GBSP can be targeted to place the waist exactly on surface 16.

Oper #	Type	In#	Out#	Wave	Field	StoW	W0	Target	Weight	Value	% Contrib
1: CONF	CONF	1									
2: EFLX	EFLX	4	7					0.000000	0.000000	-127.0536	0.000000
3: EFLX	EFLX	8	9					0.000000	0.000000	432.68888	0.000000
4: DIVI	DIVI	3	2					0.000000	0.000000	-3.405562	0.000000
5: RAGX	RAGX	1	1	0.000000	0.000000	1.000000	0.000000	0.000000	0.000000	0.675000	0.000000
6: RAGX	RAGX	9	1	0.000000	0.000000	1.000000	0.000000	0.000000	0.000000	2.305561	0.000000
7: DIVI	DIVI	6	5					0.000000	0.000000	3.415645	0.000000
8: GBSS	GBSS	1	16	1	1	0.000000	-0.892700	3.300000	1.000000	3.299906	50.000000
9: GBSW	GBSW	1	16	1	1	0.000000	-0.892700	3.300000	1.000000	3.299906	50.000000
10: GBSP	GBSP	1	16	1	1	0.000000	-0.892700	0.000000	1.000000	0.000000	0.000000
11: CONF	CONF	27									
12: EFLX	EFLX	4	7					0.000000	0.000000	-28.97221	0.000000
13: EFLX	EFLX	8	9					0.000000	0.000000	432.68888	0.000000
14: DIVI	DIVI	13	12					0.000000	0.000000	-14.93462	0.000000
15: RAGX	RAGX	1	1	0.000000	0.000000	1.000000	0.000000	0.000000	0.000000	0.675000	0.000000
16: RAGX	RAGX	9	1	0.000000	0.000000	1.000000	0.000000	0.000000	0.000000	10.129096	0.000000
17: DIVI	DIVI	16	15					0.000000	0.000000	15.006068	0.000000
18: GBSS	GBSS	1	16	1	1	0.000000	-0.487700	7.300000	1.000000	7.300000	2.14E-012
19: GBSW	GBSW	1	16	1	1	0.000000	-0.487700	7.300000	1.000000	7.300000	2.14E-012
20: GBSP	GBSP	1	16	1	1	0.000000	-0.487700	0.000000	0.000000	0.000000	0.000000

Table 8. Merit Function spreadsheet in Zemax showing the outer configurations 1 and 9 for the y-beam expander. The GBSS, GBSW, and GBSP operands target the Gaussian beam ½-diameter in this case on surface 15 (not 16), which is the required location for the re-imaged y-beam waist. Note also every parameter is defined in terms of y here, not in terms of x as in Table 7.

Oper #	Type	In#	Out#	Wave	Field	StoW	W0	Target	Weight	Value	% Contrib
1: CONF	CONF	1									
2: EFLY	EFLY	8	9					0.000000	0.000000	432.68888	0.000000
3: EFLY	EFLY	10	13					0.000000	0.000000	-1455.080	0.000000
4: DIVI	DIVI	3	2					0.000000	0.000000	-3.362878	0.000000
5: RAGY	RAGY	1	1	0.000000	0.000000	0.000000	1.000000	0.000000	0.000000	0.675000	0.000000
6: RAGY	RAGY	14	1	0.000000	0.000000	0.000000	1.000000	0.000000	0.000000	2.163800	0.000000
7: DIVI	DIVI	6	5					0.000000	0.000000	3.205630	0.000000
8: GBSS	GBSS	1	15	1	1	0.000000	0.892700	3.180000	1.000000	3.180002	50.000000
9: GBSW	GBSW	1	15	1	1	0.000000	0.892700	3.180000	1.000000	3.180002	50.000000
10: GBSP	GBSP	1	15	1	1	0.000000	0.892700	0.000000	0.000000	0.000000	0.000000
11: CONF	CONF	9									
12: EFLY	EFLY	8	9					0.000000	0.000000	432.68888	0.000000
13: EFLY	EFLY	10	13					0.000000	0.000000	-2322.144	0.000000
14: DIVI	DIVI	13	12					0.000000	0.000000	-5.366776	0.000000
15: RAGY	RAGY	1	1	0.000000	0.000000	0.000000	1.000000	0.000000	0.000000	0.675000	0.000000
16: RAGY	RAGY	14	1	0.000000	0.000000	0.000000	1.000000	0.000000	0.000000	3.562818	0.000000
17: DIVI	DIVI	16	15					0.000000	0.000000	5.278249	0.000000
18: GBSS	GBSS	1	15	1	1	0.000000	0.600000	3.180000	1.000000	3.180000	1.29E-012
19: GBSW	GBSW	1	15	1	1	0.000000	0.600000	3.180000	1.000000	3.180000	1.29E-012
20: GBSP	GBSP	1	15	1	1	0.000000	0.600000	0.000000	0.000000	0.000000	0.000000

We can now look at the final motions of the lens elements and note that indeed they fit within the required space constraints.

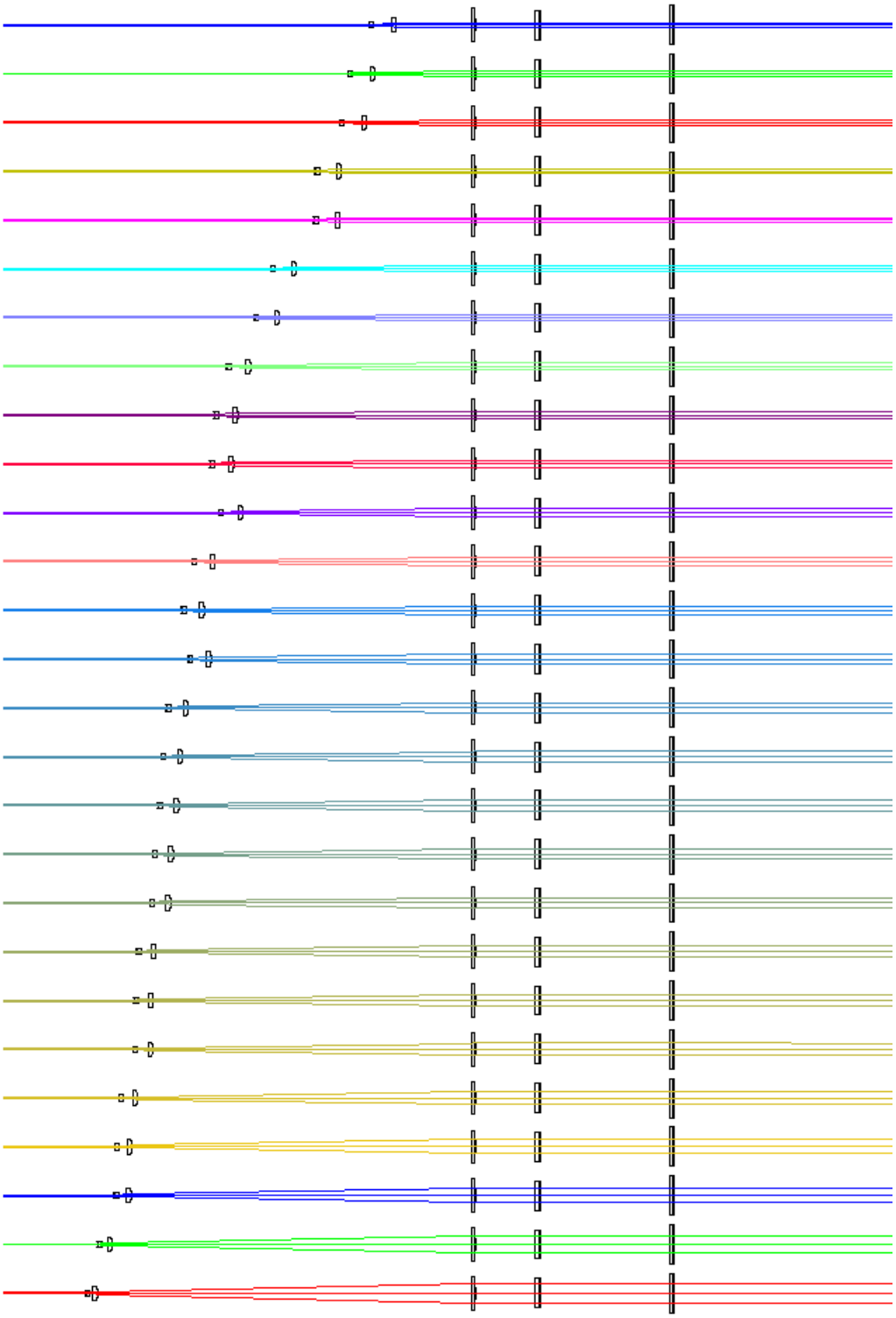

Figure 4. Layout of the x-beam expander's 27 configurations showing the motions of E1 and E2 with respect to the stationary E3. E4 and E5 are set to a nominal position and are not moving.

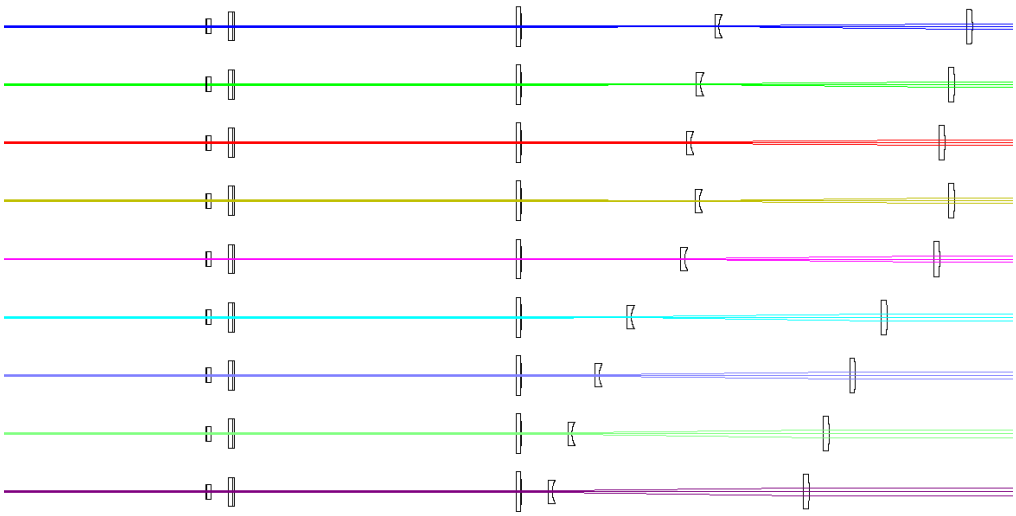

Figure 5. Layout of the y-beam expander's 9 configurations showing the motions of E4 and E5 with respect to the stationary E3. E1 and E2 are set to a nominal position and are not moving.

4. MECHANICAL DESIGN

4.1 Mechanical implementation

The mechanical design of the beam expander can be broken down into three areas:

1. Linear Guide System
2. Actuators and Feedback
3. Element Mounts

The entire system must fit within the 850mm overall length as previously defined and operate within a fairly narrow space inside the LDI illumination system. These constraints on the operating envelope play a significant role in defining the final mechanical implementation.

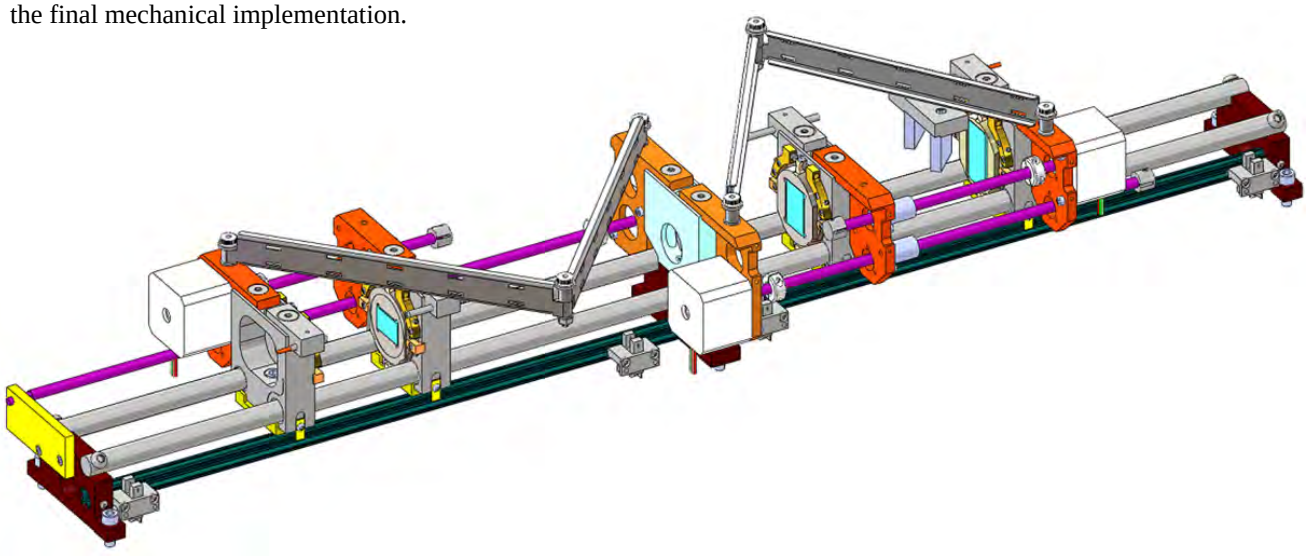

Figure 6. Motorized x,y-beam expander assembly. The element cells are labeled from left to right as E1, E2, E3, E4, and E5. E1 and E2 are able to slide along the entire length of the guide rods between the left hard stop and E3, while E4 and E5 are able to slide along the entire length of the guide rods between E3 and the right hard stop.

4.2 Linear Guide System

The linear motion zoom positions of the four moving elements require long travel distance, high resolution, and a high degree of straightness. The linear guides are built using precision shafting. Precision shafting with very good straightness is readily available in customizable lengths and serves as both a structural element and the datum system for the assembly. Each of the lens elements is housed in a circular sub-cell of identical diameter. The diameters are chosen such that when the cells are in contact with (tangent to) the surface of the guide rails, the optical centerlines will be coincident.

The central spherical element E3 is in a fixed location, while the other four elements translate along the rods. Linear bushings are designed into carriers which hold the sub-cells and drive the system components. Given the precision fit between the bushings and the rods, a flexure feature is added to the carriers to prevent the possibility of binding from an over-constrained condition.

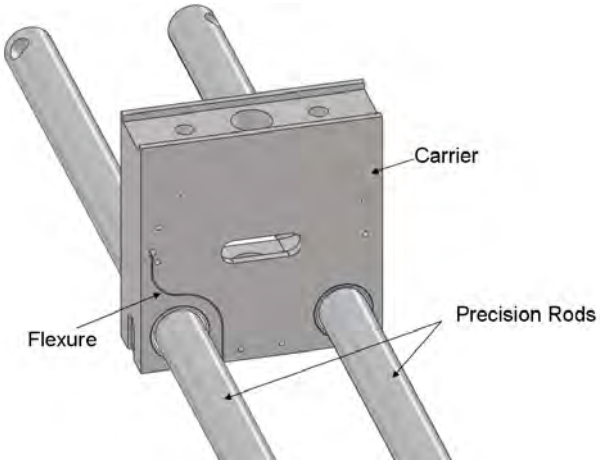

Figure 7. Cell carrier with linear bushings.

Since the rods define not only the linear motion, but also act as the support structure for the carriers, it is necessary to verify through analysis that the rods will provide sufficient rigidity to prevent resonances below a predefined limit established for all systems within the LDI tool. Finite Element Analysis is used to analyze a simplified structural model of the worst case configuration, which is a position where the two moving elements of the x-beam expander are in close proximity to each other and at roughly the half-way point in their travel. The FEA results of this position are used to determine the rod diameter to provide the necessary rigidity without adding more mass and cost than necessary.

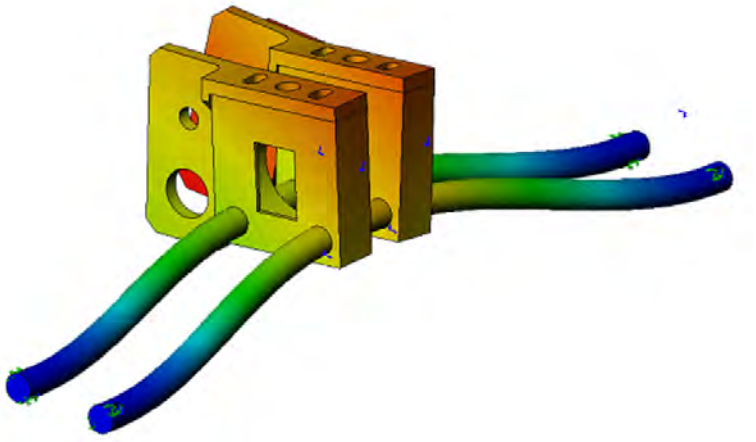

Figure 8. FEA modal analysis of the worst case carrier positions at the center of their travel.

4.3 Actuators and Feedback

To meet the requirement for remote adjustability, we use stepper motors as the basis of the drive system for the linear actuators. Stepper motors are straightforward to control and can be driven reliably in open loop, as long as sufficient motor force is available to eliminate the risk of stalling and lost counts (i.e. drive pulses counted but not resulting in the expected motor rotation). Hayden™ Hybrid Linear Actuators are available in standard hybrid stepper motor sizes integrated with lead screw assemblies. The assemblies are also available in low-outgassing/clean versions that are well suited to the LDI application.

As discussed in Section 3 on Optical Design, the x,y-magnification and waist positions are set by independently driving each of the cylindrical elements independently. To accomplish this in the minimum space envelope, two liner actuators are mounted to the fixed central point within the assembly that also houses the spherical element. One of these actuators moves the x-group of E1 and E2 together relative to the fixed E3, thereby setting the distance from E1 to E3. The second actuator moves in similar fashion the y-group of E4 and E5 together relative to the fixed E3, thereby setting the distance from E3 to E5. The third actuator is mounted to E1, with the lead screw connected to E2, thereby setting the distance between both E2 and E3. In similar fashion, a fourth actuator is mounted to E5, with the lead screw connected to E4, thereby setting the distance between both E3 and E4.

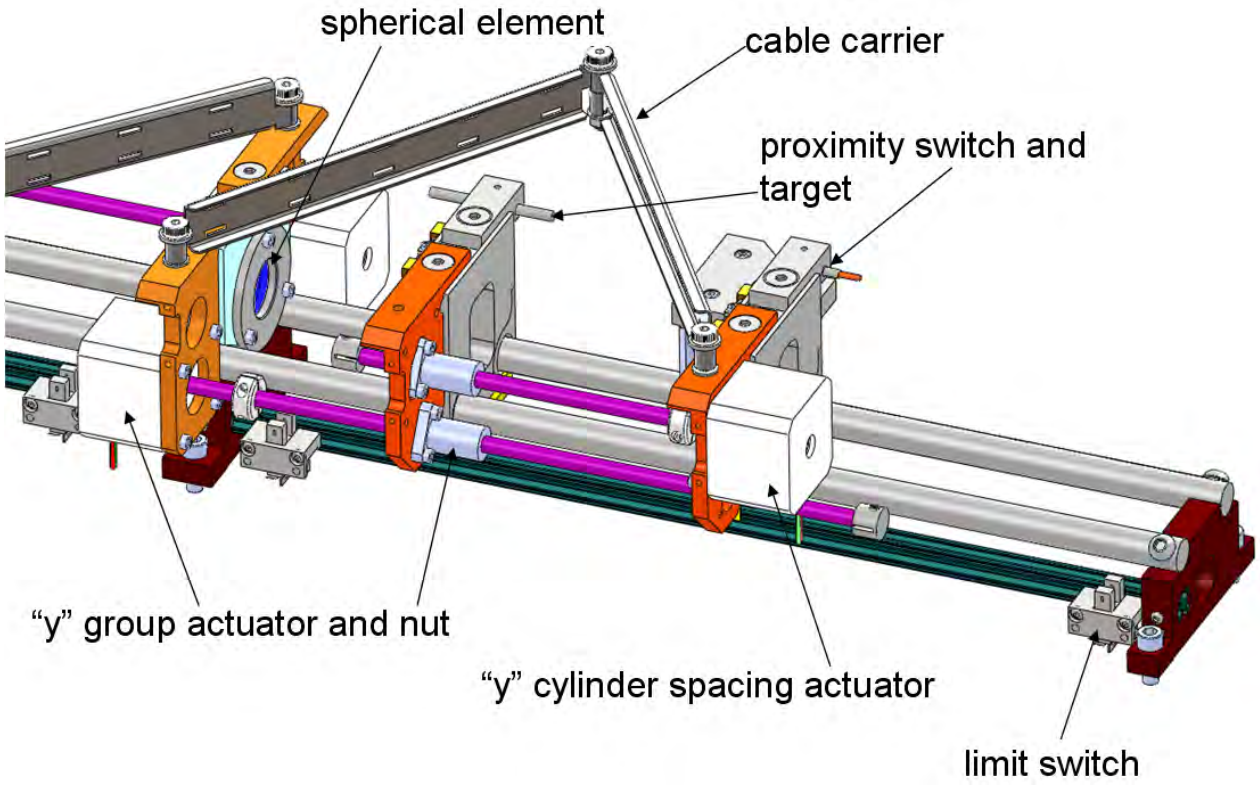

Figure 9. y-beam expander E3, E4, and E5 showing the two actuators and feedback sensors.

To facilitate homing and prevent possible mechanical collisions from occurring, homing and limit switches are added to the assembly. Infrared photo-interrupt style switches are used to set the limits of the groups on the rail, and miniature proximity switches are used to home the distance between the cylindrical elements.

4.4 Element mounts

In order for the beam expander to function properly, it is necessary for the cylindrical elements to be very well aligned relative to each other. Initially we conceived of and tested a method of passive alignment by mounting the optical surface of each element directly on a precision linear seat; however, we found that both short and long radii of curvatures would not achieve accurate enough alignment of the cylinders (it does work reasonably well for medium radii). Since the beam expander has one strong, one weak, and two medium powered elements, the mounts were re-designed to allow for all four elements to be actively aligned to meet the demanding requirements of the assembly.

The active alignment of the cylinders is accomplished through the following steps:

1. The cylinder is potted into a predominantly circular sub-cell, such that the plano surface of the cylindrical element is parallel to the datum surface of the cell, and the optical axis of the cylinder is coincident with the axis of the cell.

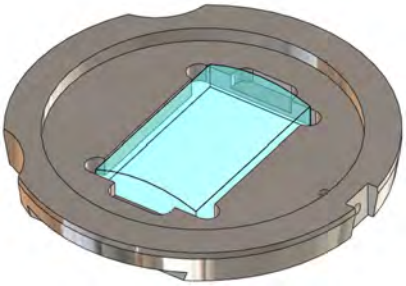

Figure 10. Sample sub-cell for E2 and E4, the medium powered elements.

2. The cell is mounted into a carrier and centered relative to the carrier datums. The nominal position of the cell is defined by the position where the outer diameter of the cell is tangent to the precision rods passing through the linear bushings.
3. The cell is then rotated in the carrier, such that the power axis of the cylinder is oriented to a tight tolerance relative to the cell datums.

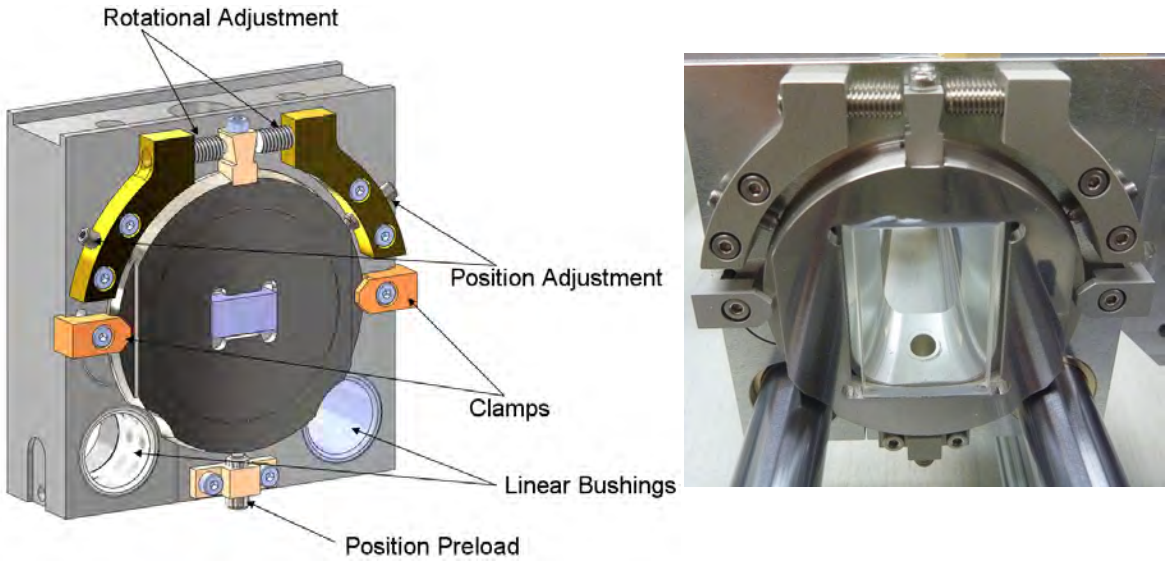

Figure 11. Carrier assemblies holding sub-cell for E1 / E4 with primary features indicated. Tightening the clamps against the element cell effectively locks both the rotation and position and creates a rigid assembly resistant to shock and vibration. Each of the carriers is assembled and aligned utilizing dedicated fixturing to ensure consistent results.

5. PROTOTYPE PHOTOS

5.1 Mounted carriers for E1 and E2

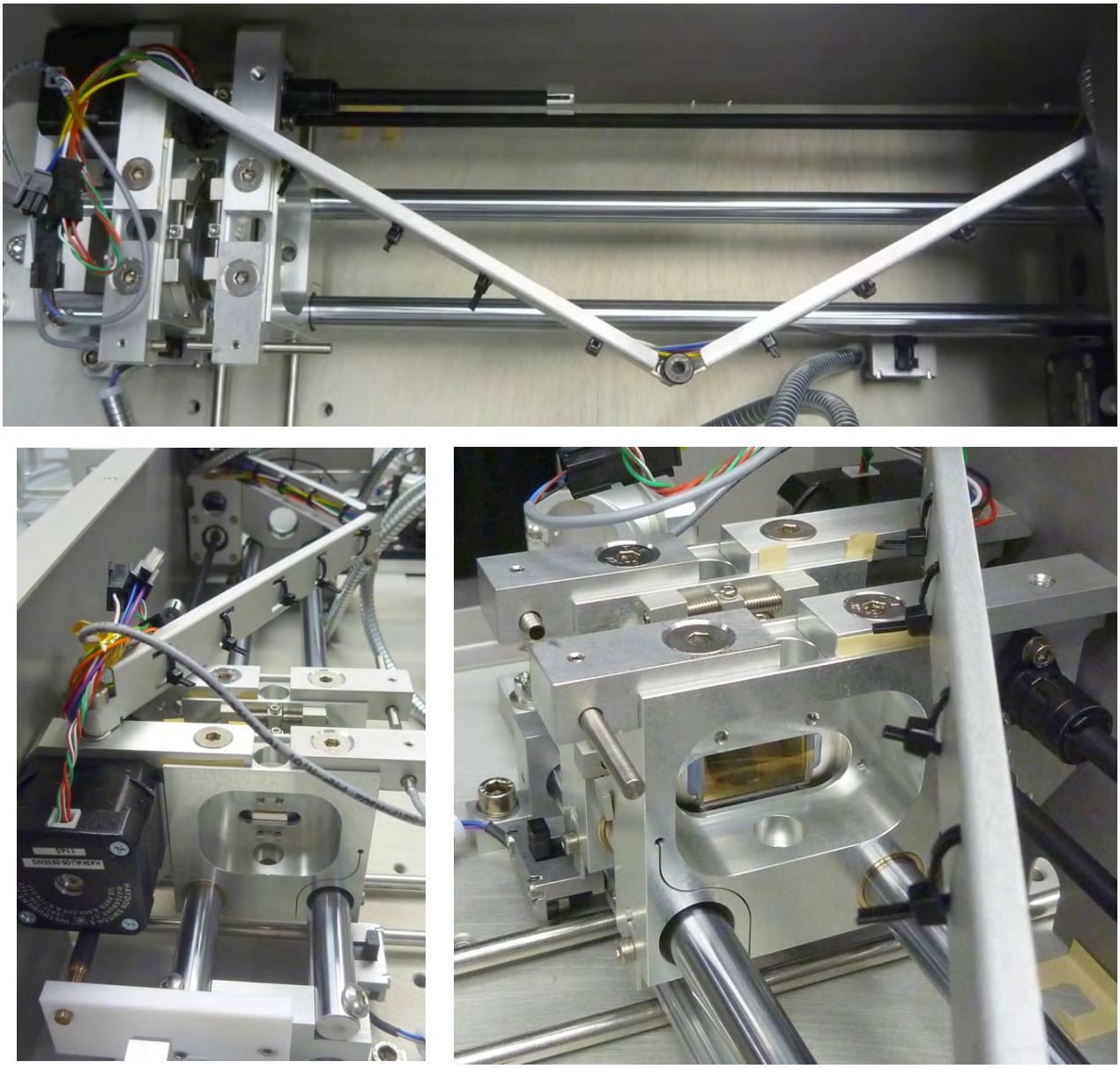

Figure 12. Top, front, and rear views of E1 and E2 carriers. Rails, motors, lead screws, limit switches, proximity switches, and E3 all visible.

5.2 Mounted carriers for E4 and E5

Figure 13. Top, front, and rear views of E4 and E5 carriers. Rails, motors, lead screws, limit switches, proximity switches, and E3 all visible.

6. CONCLUSIONS

We have successfully designed, fabricated, and tested a motorized variable anamorphic beam expander optimized for the specific beam parameters of a high power 355 nm UV laser. The beam expander can adjust the x- and y- output beam characteristics independently. In particular, the x- and y-magnification and re-imaging of the x- and y-beam waists to specific locations are incorporated in the design to ensure proper functionality of a complex illumination system further downstream. The mechanical implementation incorporates a variety of innovative mounting and linear actuation features which make the opto-mechanical system non-traditional yet robust. Serial production is planned in the near future.

ACKNOWLEDGEMENTS

The authors wish to thank Nate Burdick of ASE Optics for his assistance in developing the initial optical concept and recognizing the laser beam input parameter ranges. Vlad Kasha of CVI Melles Griot assisted significantly in the mechanical design of the lens element mounts. We also gratefully appreciate the contributions of Andrzej Karawajczyk of Micronic Mydata for the many insightful discussions and overall guiding force behind this project.

REFERENCES

[1] Choi, J.H., "Some Fundamental Aspects of UV Laser Direct Imaging," Circuit World 21(4), 18-21 (1995).
[2] Pflanz, T., "Solid-State UV Lasers Enable Laser Direct Imaging," EuroPhotonics, Dec/Jan, (2008).
[3] Mond, M., Schoene, H., Diening, A., Hollemann, G., Seelert, W., "Highly Stable UV-Mode-Locked Lasers with an Output Power of 35 W at 355 nm," Proc. SPIE 7193, Solid State Lasers XVIII: Technology and Devices (2009).
[4] , "Paladin Advanced 355 Data Sheet," http://www.coherent.com/products/?676/Paladin-Family-of-UV-Lasers (2009).
[5] , "Gaussian Beam Optics," CVI Melles Griot Technical Guide, http://www.cvimellesgriot.com/Products/Documents/TechnicalGuide/Gaussian-Beam-Optics.pdf (2010).
[6] Self, S., "Focusing of spherical Gaussian beams," Applied Optics 22(5), 658-661 (1983).
[7] Herloski, R., Marshall, S., Antos, R., "Gaussian beam ray-equivalent modeling and optical design," Applied Optics 22(8), 1168-1174 (1983).
[8] Product and Registered Trademark of Radiant Zemax LLC, www.radiantzemax.com .